ACS Photonics

Article

pubs.acs.org/journal/apchd5

Efficient Multiterminal Spectrum Splitting via a Nanowire Array Solar Cell

Alexander Dorodnyy,*[,†] Esther Alarcon-Lladó,[‡] Valery Shklover,[§] Christian Hafner,[†] Anna Fontcuberta i Morral,[‡] and Juerg Leuthold[†]

[†]Institute of Electromagnetic Fields, ETH Zurich, 8092 Zurich, Switzerland

[‡]Laboratory of Semiconductor Materials, EPFL Lausanne, 1015 Lausanne, Switzerland

[§]Laboratory of Crystallography, ETH Zurich, 8093 Zurich, Switzerland

Supporting Information

ABSTRACT: Nanowire-based solar cells opened a new avenue for increasing conversion efficiency and rationalizing material use by growing different III−V materials on silicon substrates. Here, we propose a multiterminal nanowire solar cell design with a theoretical conversion efficiency of 48.3% utilizing an efficient lateral spectrum splitting between three different III−V material nanowire arrays grown on a flat silicon substrate. This allows choosing an ideal material combination to achieve the proper spectrum splitting as well as fabrication feasibility. The high efficiency is possible due to an enhanced absorption cross-section of standing nanowires and optimization of the geometric parameters. Furthermore, we propose a multiterminal contacting scheme that can be fabricated with a technology close to standard CMOS. As an alternative we also consider a single power source with a module level voltage matching. These new concepts open avenues for next-generation solar cells for terrestrial and space applications.

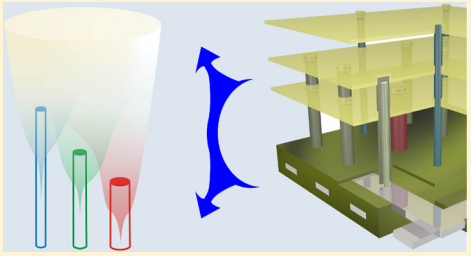

KEYWORDS: *photovoltaics, nanowire, spectrum splitting, photonic crystals*

Introducing multiple band gap concepts into nanowire solar cell designs has high promise for maximum solar conversion efficiency while keeping the unique advantages of the nanowires. Nanowire-based solar cells are increasingly attracting attention due to their enhanced absorption properties and the possibility to combine a wide selection of different materials.[1−8] The nanowire geometry allows them to be used in various ways from vertical[9] or horizontal[10] arrangements to hybrid cells comprising organic materials.[11−14] The diameter of a nanowire is much smaller than its length, so that defect-free nanowires can be grown on substrates with lattice constants considerably different from their own.[15−17] As a result, silicon and III−V materials can be combined in a double-junction cell.[18,19] The geometry of nanowires also allows engineering light−matter interactions to obtain enhanced absorption combined with antireflection properties.[20−23] Various nanowire-based solar cell designs have been proposed. The profound understanding of the photonic properties of standing nanowires resulted in an experimental realization of a single-junction InP nanowire cell reaching 13.8% efficiency.[4] Various designs suggest that the cells can be improved by using dual-junction nanowires with axial or radial junctions,[24−26] by an additional junction in the substrate,[26,27] by heterojunction with organic semiconductors,[11−13] etc. It was also predicted that efficiencies above 39% for double-junction nanowire designs should be feasible.[24] With all the work done however the pool of possibilities and concepts leading to principally new efficient solar cell designs that utilize nanowires is far from being depleted. For example, the spectrum splitting, a natural way to increase a photovoltaic conversion system efficiency,[28,29] has found yet a very limited application in nanowire solar cell concepts. Spectrum splitting allows reducing the carrier thermalization loss and thereby greatly improving the conversion efficiency of each photon.[30,31] The efficiency of classical multijunction cells (the most common cells utilizing the spectrum splitting) has recently reached 44.7%.[32] For the nanowires it was suggested to use core−shell[24] or axial[26] tandem structures. The issue however is that such designs require a fabrication of tunnel junctions in dissimilar materials, which has proven to be extremely challenging.[33,34] In addition, the performance of these cells is limited by the current-matching condition.

The questions we address in this work are the following: Should one be bound to the classical multijunction design[32] and replicate it directly on each nanowire?[24,26] Is it possible to think outside the box and to lay out new arrangements of nanowires that act effectively like a multijunction device, just by considering their special photonic properties?

MULTITERMINAL NANOWIRE ARRAY

In this paper we present a novel nanowire-based triple band gap design with a two-dimensional spatial arrangement of three independently contacted nanowire subarrays grown on a single

Received: April 26, 2015
Published: July 31, 2015

DOI: 10.1021/acsphotonics.5b00222
ACS Photonics 2015, 2, 1284−1288

flat substrate. The design combines all the advantages of the spectrum splitting with independent subcell contacting and fabrication on a silicon substrate. Nanowires allow one to combine a wide range of materials such as growing III−V nanowires on a silicon substrate[3,15,17,35] and to simultaneously grow different nanowires on the same substrate.[35,36] From the detailed balance consideration we chose $Al_{0.54}Ga_{0.46}As$, GaAs, and $In_{0.37}Ga_{0.63}As$ so that they form an ideal band gap combination (2.01, 1.42, and 0.93 eV, correspondingly). These materials can be grown in the same epitaxial system, which is important for the fabrication process. The nanowires of different materials are physically separated, so that the complexity of each wire is not greater than that in a single-junction nanowire design. This makes the fabrication of such nanowires much easier than, for example, double-junction nanowires, which additionally require a tunnel junction.[24,26] The spectrum splitting and the independent electrical connection of the subarrays bring a high conversion efficiency and great spectrum change tolerance (due to the absence of current and voltage matching limitations; see Supporting Information section 1). To allow independent connections, the substrate must have three independent contact grids, one for each nanowire subarray. The latter can be realized by a layered structure of highly doped silicon conduction lines within an insulating silicon dioxide substrate fabricated with a CMOS-like technology (see Figure 1). We should note here

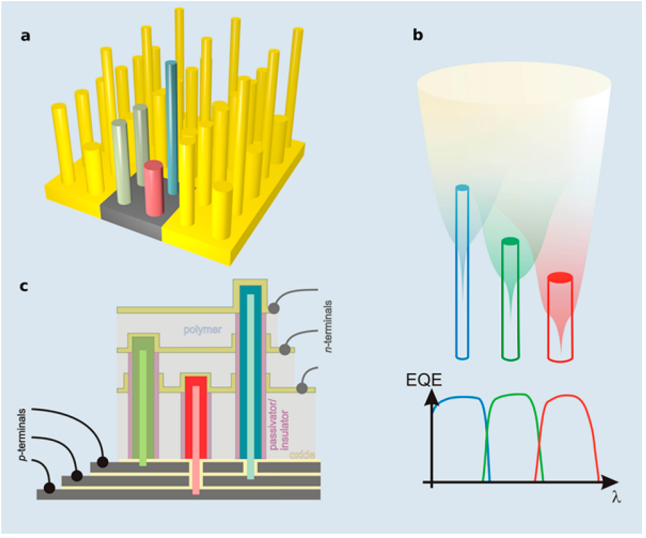

Figure 1. Design concept. (a) Schematic illustration of the triple-junction nanowire array on a Si substrate. Each unit cell contains high, low, and two medium band gap nanowires (the higher the band gap value, the higher the wires). (b) Working principle of the design. (c) Contacting scheme of the multiterminal device. Photoelectrical power is extracted separately from nanowires of different band gaps (lengths), so that the generated power is directly added.

that we suggest using radial junction nanowires so that the silicon conduction lines will be contacting the cores of the corresponding nanowires while the shells will be connected by transparent contacts (see Supporting Information section 3 for a detailed description).

Figure 1 shows the general scheme, working principle, and contacting scheme for the triple-junction nanowire array proposed in this work. Nanowires made of materials with different band gaps are arranged on the substrate in a two-dimensional periodic array such that the incoming light is absorbed selectively within the wires according to the band gap. As a general rule, the larger the band gap, the taller the nanowires should be. The idea here is that high-energy photons will be completely absorbed before they reach the height of nanowires with a lower band gap (see Figure 1b). This is due to the advantage of the increased absorption cross-section in standing nanowires. As a result, the solar spectrum is divided into three absorption spectral ranges. The periodic array has a rectangular unit cell, where the higher and lower band gap nanowires are disposed on one side of the cell, while the nanowires with a medium band gap are arranged on the other side (see Figure 1a). Simulations indicate that the best performance is achieved with two medium band gap nanowires per unit cell. This configuration was chosen over others because it has a similar or superior performance with a simpler geometry and fewer parameters. In particular we performed a short set of comparisons for several hexagonal arrangements and rectangular unit cells. Similar results were obtained for most of the configurations. Thus, we focus on the simplest rectangular unit cell with a rectangular arrangement of nanowires inside. For this arrangement it is natural that one of the nanowire types is duplicated within the cell in order to achieve an efficient space utilization. The GaAs nanowires were chosen to be doubled because they provide the highest contribution to the efficiency, arising from light absorption closest to the maximum of the solar spectrum. A more detailed study of different nanowire arrangements is very time-consuming and will be performed in future works.

The optimized structure has the following parameters: $Al_{0.54}Ga_{0.46}As$, GaAs, $In_{0.37}Ga_{0.63}As$ nanowire radii (lengths) of 51 nm (12 μm), 73 nm (6.6 μm), and 114 nm (3.3 μm), respectively, array periods of 580 × 500 nm, and center-to-center spacing between GaAs−GaAs (GaAs−InGaAs) nanowires of 290 nm (250 nm). The equivalent bulk thicknesses of AlGaAs, GaAs, and InGaAs layers are 340, 760, and 460 nm, correspondingly. The lengths, diameters, and positions of the nanowires are calculated and optimized using a Fourier modal method (FMM)[37] combined with an evolution strategy (ES)[38] and Nelder−Mead[39] optimizers (see Supporting Information section 2 for more details). We present here the calculations for a triple band gap solar cell, but the principle can be employed for a higher number of junctions.

Figure 1c depicts a contacting scheme of the three solar subcells. The junctions are designed in a core−shell fashion. The core−shell structures offer more robustness in terms of surface recombination losses. Still, axial junctions would also be possible if adequate surface passivation is provided. The photogenerated power is collected separately for each of the three different kinds of nanowires. Nanowires are grown on sub-micrometer-scale platforms insulated electrically from the neighboring ones. Such a scheme could be achieved by subsequently growing three nanowire subarrays on a patterned (highly doped) silicon-on-insulator substrate (SOI). The highly doped silicon platforms would directly contact nanowire cores, while nanowire shells would be contacted via transparent top-contacts. The process would involve the insulation (passivation) of the nanowires and selective etch of each of the nanowire tips, as shown in prior works.[40] A transparent polymer layer would ensure the mechanical stability of the nanowire/contacts ensemble (see Supporting Information section 3 for the detailed fabrication steps description).

DOI: 10.1021/acsphotonics.5b00222
ACS Photonics 2015, 2, 1284−1288

A natural way to collect the generated power of the multiterminal contacting scheme is to use three independent external converters supplying energy to the grid. Such schemes have a high spectrum change stability. An alternative with only one converter is a voltage matching scheme on the module level leading to a single power source. One example of such scheme with still high efficiency is presented in the Supporting Information section 4. As an advantage of such a scheme, we do not have to include tunnel junctions for current matching as in standard multijunction cells, which would make fabrication more demanding.[33,34] Although the voltage-matched scheme is less tolerant to the spectrum changes, the module interconnection scheme is very flexible. One can imagine that it could even have electronic controls that adapt to the spectrum during operation.

RESULTS AND DISCUSSION

In Figure 2a the spectral distribution of light absorption within the nanowires and detailed balance current−voltage dependences for the optimal structure are shown. The detailed balance limit efficiency estimation[41] of the optimized structure is 48.3% for an AM1.5 direct solar spectrum (see Figure 2a). This value is close to the maximum conversion efficiency for a triple band gap design under ideal sunlight splitting, which is 51.3% (for the same spectrum, see the Supporting Information section 5). One can see that the GaAs subcell gives the highest contribution to the overall conversion efficiency (see Figure 2b) and is closest to the maximum absorption within the corresponding spectral range (see Figure 2a). Such a result is to be expected due to the doubled number of GaAs nanowires compared to Al(In)GaAs. It is also beneficial from the fabrication point of view because the GaAs is a simple compound material and the least demanding in the growth process. Furthermore, the GaAs single-junction cell showed 28.8% efficiency,[42] which is close to the detailed balance conversion efficiency. The highest yield subcell in the design is therefore also the most promising from the fabrication point of view. Another observation one can make from Figure 2a is that the majority of the absorption losses are happening at the beginning and at the end of the absorption range. The loss at the beginning (low frequencies) happens due to the low absorptivity of InGaAs close to its band gap. That could be compensated by increasing the lengths of the corresponding nanowires or a choice of material with a steeper absorption growth near the band gap. The loss at the end (high frequencies) happens due to the cross-section of AlGaAs nanowires reaching its limits. At high frequencies the wavelength of the light becomes smaller than the internanowire distance and some photons are passing through without feeling the nanowires' presence. Both of the issues listed above will become a subject of further research on improved material combinations and nanowire array geometries.

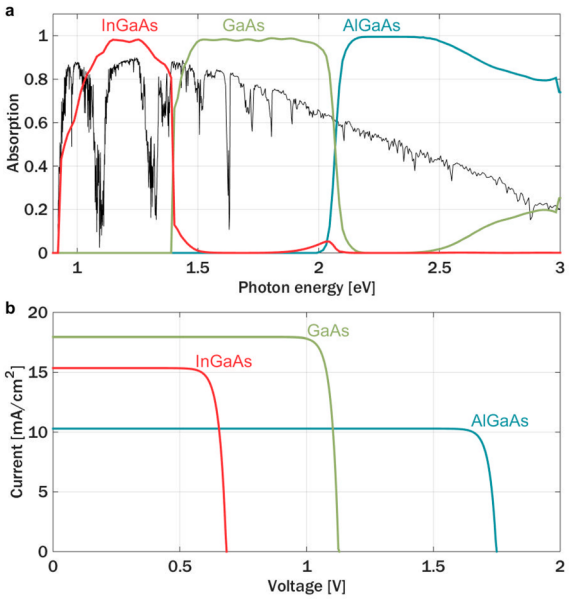

Figure 2. Performance calculation. (a) Absorption distribution between the different band gaps. (b) Current−voltage dependences of the optimal nanowires' structure. Calculations are made using detailed balance limit and AM1.5 direct solar spectrum. Overall efficiency limit of the nanowire array is 48.3%. Current/voltage (in mA/cm^2 and V) in the optimal points for $Al_{0.54}Ga_{0.46}As$ is 10.1/1.64, for GaAs, 17.5/1.03, and for $In_{0.37}Ga_{0.63}As$, 14.7/0.60.

The obtained result (48.3% out of a maximal 51.3% detailed balance efficiency) shows a high potential of the optical design due to the nanowire concentration effect. It is evident though that a more realistic conversion efficiency could be obtained with a more detailed consideration of factors such as nonradiative losses, resistive losses, and additional losses introduced by transparent contacts. To get a hint about the fabrication demands and resistive losses of the designed cell, one can consult the band profile estimations for nanowires performed in ref 43. We will take the AlGaAs wires as an example. Due to these nanowires being the thinnest and longest, the corresponding subcell will certainly exhibit the highest series resistance and voltage reduction. We assume core and shell doping levels of $n = 10^{19}$ cm^{-3} and a surface-state density below 10^{11} cm^{-2} eV^{-1}. For the nanowires with a diameter of around 100 nm we can estimate from ref 43 that it is possible to have a partially nondepleted core and shell, which is essential for the conductivity. Due to the smaller mobility of free holes, we address here the voltage drop given in the p-type core of the AlGaAs nanowires. For 54% of aluminum the hole mobility is expected to be around $\mu_h = 54$ cm^2/V/s. The nondepleted (conductive) section roughly corresponds to half of the nanowire cross-section, $S = 0.5\pi r^2 = 3.93 \times 10^{-11}$ cm^2. Thus, the resistance at the nanowire core will be $R = l/(n\mu_h eS) = 353$ kΩ, where $l = 12$ μm is the nanowire length. Under the one sun operation conditions, the current flowing through the AlGaAs nanowire will be $I = 2.93 \times 10^{-11}$ A. Thus, the voltage drop due to the core resistance will be $dV = IR = 3 \times 10^{-5}$ V. In conclusion, the series resistance for a realistic device should not degrade too much the theoretical values, provided that there is an impeccable fabrication protocol. It is also worth mentioning that the surface recombination is less critical for radial junctions.[44]

The actual efficiency that would be obtained experimentally depends on multiple parameters, some of which depend strongly on the fabrication process (such as defect densities). However, a rough estimation of efficiency can be given based on the known technological achievements. As described in ref 45, we can assume that recombination in GaAs-based III−V materials is around 150 times stronger than its radiative values, and therefore the actual efficiency would be around 42% rather than 48%.

To further illustrate the working principle of our design, we show how the light is spatially distributed and selectively

DOI: 10.1021/acsphotonics.5b00222
ACS Photonics 2015, 2, 1284−1288

absorbed in the nanowire array. In Figure 3 we depict the Poynting vector flow-lines near the nanowires for photon

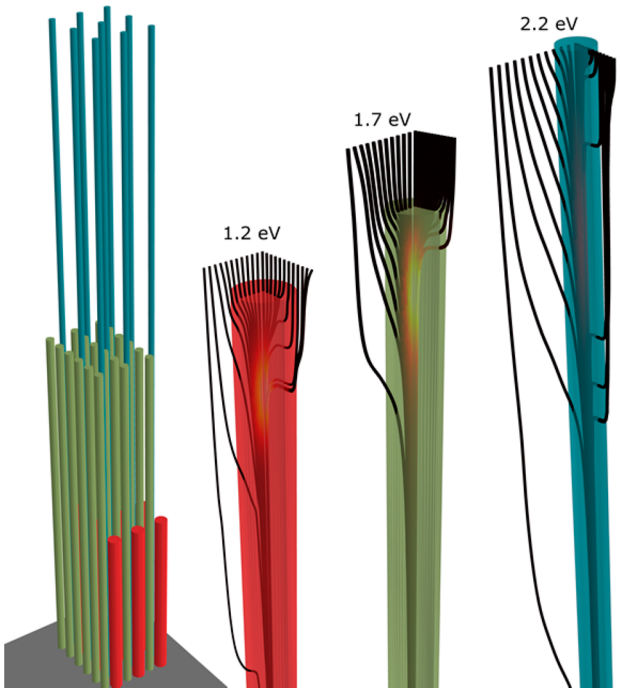

Figure 3. Poynting vector flow-lines for frequencies of 1.2, 1.7, and 2.2 eV. Each distribution is shown near a nanowire with an appropriate band gap. The nanowire array structure shown here is the optimal design found from the optimization.

energies of 1.2, 1.7, and 2.2 eV. The Poynting vector is a direct illustration of the electromagnetic energy flow. Calculations shown in Figure 2a indicate that for all of the absorbed photon energies not only does light enter the nanowire through the top surface, but the Poynting vector gradually leads in through the side walls. This is a consequence of the nanowire light concentration. The pattern of energy flow is key to the efficient spectral light splitting within the nanowire array. In this way high-frequency photons (above the AlGaAs band gap) are being mostly absorbed before reaching the GaAs nanowires, and in the same way medium-frequency photons (above the GaAs and below the AlGaAs band gap) are being absorbed by GaAs nanowires before reaching InGaAs.

CONCLUSION

In conclusion, a new strategy for the design of highly efficient nanowire-based solar cells is outlined. We propose splitting the incoming solar spectrum spatially so that nanowires with different band gaps separately photoconvert it into electrical power. This opens new possibilities for multijunction cells, where materials with different band gaps and lattice constants are combined on a single substrate. The physically separated junctions based on nanowires guarantee spatial solar spectrum splitting while avoiding the need to fabricate complicated nanowires with tunnel junctions. The absence of the current/voltage matching limitations results in an extremely high theoretical conversion efficiency, namely, 48.3% without light concentration. The design ensures a significantly reduced material consumption compared to standard bulk structures due to the low nanowire volume and the fabrication on a silicon substrate. Although the fabrication and contacting scheme are challenging, we propose that current CMOS technology processes could be transferred to this kind of device. Finally, independent contacting of different junctions grants improved spectrum stability, compared to current matched schemes. This novel nanowire-based multi-band-gap solar cell scheme opens the path toward a new generation of devices that fully exploit the potential of nanowires.

ASSOCIATED CONTENT

Supporting Information

The Supporting Information is available free of charge on the ACS Publications website at DOI: 10.1021/acsphotonics.5b00222.

Proposed fabrication process and contacting arrangement as well as detailed description of simulation and optimization techniques (PDF)

AUTHOR INFORMATION

Corresponding Author

*E-mail: dorodnya@ethz.ch.

Notes

The authors declare no competing financial interest.

ACKNOWLEDGMENTS

The authors are indebted to Swiss National Science Foundation (project 143908 "Light trapping enhanced mesoscopic solar cells"), Ambizione Energy PZENP2_154283, ERC StG UpCon, NanoTera Synergy, ITN Nanoembrace, and Zero-power.

REFERENCES

(1) Zeng, Y.; Ye, Q. H.; Shen, W. Z. Design principles for single standing nanowire solar cells: going beyond the planar efficiency limits. *Sci. Rep.* **2014**, *4*, 4915.

(2) Callahan, D. M.; Munday, J. N.; Atwater, H. A. Solar Cell Light Trapping beyond the Ray Optic Limit. *Nano Lett.* **2012**, *12*, 214−218.

(3) Krogstrup, P.; Jorgensen, H. I.; Heiss, M.; Demichel, O.; Holm, J. V.; Aagesen, M.; Nygard, J.; Morral, A. F. I. Single-nanowire solar cells beyond the Shockley-Queisser limit. *Nat. Photonics* **2013**, *7*, 306−310.

(4) Wallentin, J.; Anttu, N.; Asoli, D.; Huffman, M.; Aberg, I.; Magnusson, M. H.; Siefer, G.; Fuss-Kailuweit, P.; Dimroth, F.; Witzigmann, B.; Xu, H. Q.; Samuelson, L.; Deppert, K.; Borgstrom, M. T. InP nanowire array solar cells achieving 13.8% efficiency by exceeding the ray optics limit. *Science* **2013**, *339*, 1057−60.

(5) Garnett, E. C.; Yang, P. D. Silicon nanowire radial p−n junction solar cells. *J. Am. Chem. Soc.* **2008**, *130*, 9224−9225.

(6) Kelzenberg, M. D.; Boettcher, S. W.; Petykiewicz, J. A.; Turner-Evans, D. B.; Putnam, M. C.; Warren, E. L.; Spurgeon, J. M.; Briggs, R. M.; Lewis, N. S.; Atwater, H. A. Enhanced absorption and carrier collection in Si wire arrays for photovoltaic applications. *Nat. Mater.* **2010**, *9*, 239−244.

(7) Kempa, T. J.; Cahoon, J. F.; Kim, S. K.; Day, R. W.; Bell, D. C.; Park, H. G.; Lieber, C. M. Coaxial multishell nanowires with high-quality electronic interfaces and tunable optical cavities for ultrathin photovoltaics. *Proc. Natl. Acad. Sci. U. S. A.* **2012**, *109*, 1407−1412.

(8) Ji, S.; Ye, C. Cu_2ZnSnS_4 as a New Solar Cell Material: The History and the Future. *Rev. Adv. Sci. Eng.* **2012**, *1*, 42−58.

(9) Rao, H. S.; Wu, W. Q.; Liu, Y.; Xu, Y. F.; Chen, B. X.; Chen, H. Y.; Kuang, D. B.; Su, C. Y. CdS/CdSe co-sensitized vertically aligned anatase TiO2 nanowire arrays for efficient solar cells. *Nano Energy* **2014**, *8*, 1−8.

(10) Choi, H.; Radich, J. G.; Kamat, P. V. Sequentially Layered CdSe/CdS Nanowire Architecture for Improved Nanowire Solar Cell Performance. *J. Phys. Chem. C* **2014**, *118*, 206−213.

DOI: 10.1021/acsphotonics.5b00222
ACS Photonics 2015, 2, 1284−1288

(11) Ben Dkhil, S.; Ebdelli, R.; Dachraoui, W.; Faltakh, H.; Bourguiga, R.; Davenas, J. Improved photovoltaic performance of hybrid solar cells based on silicon nanowire and P3HT. *Synth. Met.* **2014**, *192*, 74−81.
(12) Wang, W. B.; Li, X. H.; Wen, L.; Zhao, Y. F.; Duan, H. H.; Zhou, B. K.; Shi, T. F.; Zeng, X. S.; Li, N.; Wang, Y. Q. Optical simulations of P3HT/Si nanowire array hybrid solar cells. *Nanoscale Res. Lett.* **2014**, *9*, 238.
(13) Qiu, J.; Qiu, Y.; Yan, K.; Zhong, M.; Mu, C.; Yan, H.; Yang, S. All-solid-state hybrid solar cells based on a new organometal halide perovskite sensitizer and one-dimensional TiO2 nanowire arrays. *Nanoscale* **2013**, *5*, 3245−3248.
(14) Casadei, A.; Llado, E. A.; Amaduzzi, F.; Russo-Averchi, E.; Ruffer, D.; Heiss, M.; Negro, L. D.; Morral, A. F. i. Polarization response of nanowires a la carte. *Sci. Rep.* **2015**, *5*, 7651.
(15) Chuang, L. C.; Moewe, M.; Chase, C.; Kobayashi, N. P.; Chang-Hasnain, C.; Crankshaw, S. Critical diameter for III-V nanowires grown on lattice-mismatched substrates. *Appl. Phys. Lett.* **2007**, *90*, 043115.
(16) Glas, F. Critical dimensions for the plastic relaxation of strained axial heterostructures in free-standing nanowires. *Phys. Rev. B: Condens. Matter Mater. Phys.* **2006**, *74*, 121302.
(17) Fan, Z.; Razavi, H.; Do, J.; Moriwaki, A.; Ergen, O.; Chueh, Y.-L.; Leu, P. W.; Ho, J. C.; Takahashi, T.; Reichertz, L. A.; Neale, S.; Yu, K.; Wu, M.; Ager, J. W.; Javey, A. Three-dimensional nanopillar-array photovoltaics on low-cost and flexible substrates. *Nat. Mater.* **2009**, *8*, 648−653.
(18) Mallorqui, A. D.; Alarcon-Llado, E.; Russo-Averchi, E.; Tutuncuoglu, G.; Matteini, F.; Ruffer, D.; Morral, A. F. I. Characterization and analysis of InAs/p-Si heterojunction nanowire-based solar cell. *J. Phys. D: Appl. Phys.* **2014**, *47*, 394017.
(19) Kandala, A.; Betti, T.; Morral, A. F. I. General theoretical considerations on nanowire solar cell designs. *Phys. Status Solidi A* **2009**, *206*, 173−178.
(20) Ding, W. C.; Jia, R.; Li, H. F.; Chen, C.; Sun, Y.; Jin, Z.; Liu, X. Y. Design of two dimensional silicon nanowire arrays for antireflection and light trapping in silicon solar cells. *J. Appl. Phys.* **2014**, *115*, 014307.
(21) Um, H. D.; Park, K. T.; Jung, J. Y.; Li, X. P.; Zhou, K.; Jee, S. W.; Lee, J. H. Incorporation of a self-aligned selective emitter to realize highly efficient (12.8%) Si nanowire solar cells. *Nanoscale* **2014**, *6*, 5193−5199.
(22) Diedenhofen, S. L.; Janssen, O. T. A.; Grzela, G.; Bakkers, E.; Rivas, J. G. Strong Geometrical Dependence of the Absorption of Light in Arrays of Semiconductor Nanowires. *ACS Nano* **2011**, *5*, 2316−2323.
(23) Kupec, J.; Witzigmann, B. Computational electromagnetics for nanowire solar cells. *J. Comput. Electron.* **2012**, *11*, 153−165.
(24) Yu, S.; Witzigmann, B. A high efficiency dual-junction solar cell implemented as a nanowire array. *Opt. Express* **2013**, *21*, A167−A172.
(25) Kempa, T. J.; Tian, B. Z.; Kim, D. R.; Hu, J. S.; Zheng, X. L.; Lieber, C. M. Single and Tandem Axial p-i-n Nanowire Photovoltaic Devices. *Nano Lett.* **2008**, *8*, 3456−3460.
(26) Wen, L.; Li, X. H.; Zhao, Z. F.; Bu, S. J.; Zeng, X. S.; Huang, J. H.; Wang, Y. Q. Theoretical consideration of III-V nanowire/Si triple-junction solar cells. *Nanotechnology* **2012**, *23*, 505202.
(27) Huang, N. F.; Lin, C. X.; Povinelli, M. L. Limiting efficiencies of tandem solar cells consisting of III-V nanowire arrays on silicon. *J. Appl. Phys.* **2012**, *112*, 064321.
(28) Imenes, A. G.; Mills, D. R. Spectral beam splitting technology for increased conversion efficiency in solar concentrating systems: a review. *Sol. Energy Mater. Sol. Cells* **2004**, *84*, 19−69.
(29) Polman, A.; Atwater, H. A. Photonic design principles for ultrahigh-efficiency photovoltaics. *Nat. Mater.* **2012**, *11*, 174−177.
(30) Hirst, L. C.; Ekins-Daukes, N. J. Fundamental losses in solar cells. *Prog. Photovoltaics* **2011**, *19*, 286−293.
(31) Rau, U.; Paetzold, U. W.; Kirchartz, T. Thermodynamics of light management in photovoltaic devices. *Phys. Rev. B: Condens. Matter Mater. Phys.* **2014**, *90*, 035211.
(32) Dimroth, F.; Grave, M.; Beutel, P.; Fiedeler, U.; Karcher, C.; Tibbits, T. N. D.; Oliva, E.; Siefer, G.; Schachtner, M.; Wekkeli, A.; Bett, A. W.; Krause, R.; Piccin, M.; Blanc, N.; Drazek, C.; Guiot, E.; Ghyselen, B.; Salvetat, T.; Tauzin, A.; Signamarcheix, T.; Dobrich, A.; Hannappel, T.; Schwarzburg, K. Wafer bonded four-junction GaInP/GaAs//GaInAsP/GaInAs concentrator solar cells with 44.7% efficiency. *Prog. Photovoltaics* **2014**, *22*, 277−282.
(33) Yamaguchi, M. III-V compound multi-junction solar cells: present and future. *Sol. Energy Mater. Sol. Cells* **2003**, *75*, 261−269.
(34) Wallentin, J.; Persson, J. M.; Wagner, J. B.; Samuelson, L.; Deppert, K.; Borgstrom, M. T. High-Performance Single Nanowire Tunnel Diodes. *Nano Lett.* **2010**, *10*, 974−979.
(35) Rieger, T.; Rosenbach, D.; Mussler, G.; SchäPers, T.; Grützmacher, D.; Lepsa, M. I. Simultaneous Integration of Different Nanowires on Single Textured Si (100) Substrates. *Nano Lett.* **2015**, *15*, 1979−1986.
(36) Kakko, J.-P. P.; Haggrén, T.; Dhaka, V.; Huhtio, T.; Peltonen, A.; Jiang, H.; Kauppinen, E.; Lipsanen, H. Fabrication of Dual-Type Nanowire Arrays on a Single Substrate. *Nano Lett.* **2015**, *15*, 1679−1683.
(37) Li, L. New formulation of the Fourier modal method for crossed surface-relief gratings. *J. Opt. Soc. Am. A* **1997**, *14*, 2758−2767.
(38) Erni, D.; Wiesmann, D.; Spuhler, M.; Hunziker, S.; Moreno, E.; Oswald, B.; Frohlich, J.; Hafner, C. Application of evolutionary optimization algorithms in computational optics. *ACES J.* **2000**, *15*, 43−60.
(39) Olsson, D. M.; Nelson, L. S. Nelder-Mead Simplex Procedure for Function Minimization. *Technometrics* **1975**, *17*, 45−51.
(40) Mallorquí, A.; Alarcón-Lladó, E.; Mundet, I.; Kiani, A.; Demaurex, B.; De Wolf, S.; Menzel, A.; Zacharias, M.; Fontcuberta i Morral, A. Field-effect passivation on silicon nanowire solar cells. *Nano Res.* **2015**, *8*, 673−681.
(41) Shockley, W.; Queisser, H. J. Detailed Balance Limit of Efficiency of P-N Junction Solar Cells. *J. Appl. Phys.* **1961**, *32*, 510−519.
(42) Green, M. A.; Emery, K.; Hishikawa, Y.; Warta, W.; Dunlop, E. D. Solar cell efficiency tables (version 43). *Prog. Photovoltaics* **2014**, *22*, 1−9.
(43) Chia, A. C. E.; LaPierre, R. R. Electrostatic model of radial pn junction nanowires. *J. Appl. Phys.* **2013**, *114*, 074317.
(44) Yu, S. Q.; Roemer, F.; Witzigmann, B. Analysis of surface recombination in nanowire array solar cells. *J. Photonics Energy* **2012**, *2*, 84380O.
(45) Dorodnyy, A.; Shklover, V.; Braginsky, L.; Hafner, C.; Leuthold, J. High-efficiency spectrum splitting for solar photovoltaics. *Sol. Energy Mater. Sol. Cells* **2015**, *136*, 120−126.

DOI: 10.1021/acsphotonics.5b00222
ACS Photonics 2015, 2, 1284−1288